ELSEVIER

Contents lists available at ScienceDirect

Chemical Engineering Journal

journal homepage: www.elsevier.com/locate/cej





Assembling Nitrogen-rich, thermally Stable, and insensitive energetic materials by polycyclization

Qiong Yu^a, Jatinder Singh^a, Richard J. Staples^b, Jean'ne M. Shreeve^{a,*}

- a Department of Chemistry, University of Idaho, Moscow, ID 83844-2343 United States
- ^b Department of Chemistry, Michigan State University, East Lansing, MI 48824, USA

ARTICLE INFO

Keywords:
Polycyclization
Fused rings
Energetic materials
Insensitive
Aromaticity

ABSTRACT

In pursuit of energetic materials which have equal energies and thermal stabilities, but lower sensitivities compared with hexahydro-1,3,5-trinitro-1,3,5-triazine (RDX) and octahydro-1,3,5,7-tetranitro-1,3,5,7-tetrazocine (HMX), a new fused N-heterocyclic framework, ditriazolo-1,2,4,5-tetrazine, 7 was designed and synthesized. Compound 7 exhibits a favorable decomposition temperature of 247 °C benefiting from its good aromaticity which was studied by nucleus-independent chemical shift (NICS) and isochemical shielding surfaces (ICSS). Combined with moderate detonation properties (ν_D , 8544 m s⁻¹; P, 27.3 GPa) and low sensitivities (IS, >40 J; FS, >360 N), 7 may potentially be useful as a secondary energetic in practical applications to replace RDX. Hydrazinium salt 12 has a thermal stability of 221 °C, and excellent detonation properties (ν_D , 9088 m s⁻¹; P, 32.3 GPa), which are comparable with those of HMX. These contributions highlight the fused N-heterocyclic framework as a potential energetic backbone and provide new thinking to the chemistry of polycyclic heterocycles.

1. Introduction

Hexahydro-1,3,5-trinitro-1,3,5-triazine (RDX) and octahydro-1,3,5,7-tetranitro- 1,3,5,7-tetrazocine (HMX) continue as the most common secondary energetic materials used in military and civilian applications. The design and synthesis of new high energy dense materials have been long-standing goals. [1,2] A competitive energetic material should possess a high heat of formation and high density which give rise to good detonation properties. In addition, it should exhibit low sensitivities towards impact and friction and its thermal stability should exceed 200 °C.[3] Recently, fused cyclic energetic materials have aroused greater interest due to their inherent advantages such as high mechanical strength, thermal stability and high heat of formation, and many have been identified as promising contenders to traditional materials. [3–5] They are often large conjugate systems which contain two or more heterocyclic rings sharing two atoms and one bond between adjacent rings. Many fantastic fused tricyclic energetic materials with high nitrogen content have been explored in the efforts of energetic chemists; for example, energetic molecules such as, tetrazino-tetrazine 1,3,6,8-tetraoxide (TTTO), [6] 1,2,9,10-tetranitrodipyrazolo[1,5d:5',1'-f][1,2,3,4]tetrazine, [7] and 4-amino-3,7-dinitrotriazolo-[5,1-c]

[1,2,4] triazine (DPX-26), [8] which balance well with high performance and thermal stability, and benefit from high nitrogen content and fused ring backbones.

As part of our continuing effort to synthesize energetic high-nitrogen compounds with excellent thermostability, sensitivity, and good detonation properties, we now have designed and synthesized a fused tricyclic compound bis([1,2,4]triazolo)[4,3-b:3',4'-f][1,2,4,5]tetrazine-1,8- diamine (7), in which one tetrazine ring is conjugated with two triazole rings to give a material with a nitrogen content of 72.9% (Fig. 1). The aromaticity of 7 was studied since it is closely related to molecular planarity and various physiochemical properties (vide infra). [9] Enthalpy calculations of 7 were carried out with the Gaussian03 (Revision E.01) suite of programs. [10] Benefitting from the ring-strain energy of the fused backbone, 7 has a very high positive heat of formation of 4.27 kJ g $^{-1}$. This fused ring compound is expected to be an excellent energetic material. The product of nitration 8 and some of its salts (9–12) were also investigated to evaluate their integrated energetic performance.

E-mail address: jshreeve@uidaho.edu (J.M. Shreeve).

^{*} Corresponding author.

Fig. 1. Structures of RDX, HMX, and fused tricyclic energetic material 7.

2. Experimental

2.1. Synthesis

2.1.1. Synthesis of 6-hydrazinyl-[1,2,4]triazolo[4,3-b][1,2,4,5] tetrazin-3-amine (6)

To a slurry of 6-(3,5-dimethyl-1H-pyrazol-1-yl)-[1,2,4]triazolo[4,3-b][1,2,4,5]tetrazin-3-amine [11] (5, 2.31 g, 10 mmol) in acetonitrile (50 mL), hydrazine monohydrate (0.59 mL, 12 mmol) was added dropwise at ambient temperature. After the addition was complete, the mixture was held at reflux for 2 h. The mixture was then cooled to room temperature, filtered, and the solid was washed with acetonitrile (10 mL) to provide 6 (1.58 g, 95%) as a deep red solid. $T_{\rm d}$ (onset): 207 °C. $^{1}{\rm H}$ NMR (300 MHz, DMSO- $^{4}{\rm G}$): δ = 9.6 (s, 1H, NH), 6.9 (s, 2H, C-NH₂), 4.4 (s, 2H, N-NH₂); $^{13}{\rm C}$ NMR (75 MHz, $^{4}{\rm G}$ -DMSO): δ = 156.5 (C-NHNH₂), 148.9 (C = N), 148.7 (C-NH₂); IR (KBr): \tilde{v} =3451(s), 3351(s), 2672(w), 1685(m), 1623(s), 1490(m), 1462(w), 1401(w), 1348(m), 1142(m), 1102(m), 1050(m), 899(w), 96(w), 760(w), 670(w) cm⁻¹; Anal. calcd for $^{2}{\rm G}_{3}{\rm H}_{5}{\rm N}_{9}$: C 21.56; H 3.02; N 75.43; found: C 21.56; H 3.55; N 75.50.

2.1.2. Synthesis of bis([1,2,4]triazolo)[4,3-b:3',4'-f][1,2,4,5] tetrazine-1,8-diamine (7)

3,6-Dihydrazinyl-1,2,4,5-tetrazine[12] (2, 0.28 g, 2 mmol) was

dissolved in ethanol (10 mL), and cyanogen bromide (0.45 g, 4.2 mmol) was added. The mixture was stirred for 48 h. The yellow precipitate was filtered, washed with ethanol (3 mL) and dried in the air to yield **7** (0.29 g,75%). $T_{\rm d}$ (onset): 247 °C. ¹H NMR (300 MHz, DMSO- $d_{\rm 6}$): $\delta=7.1$ (s, 4H, NH₂); ¹³C NMR (75 MHz, DMSO- $d_{\rm 6}$): $\delta=147.8$ (C = N), 146.4 (C-NH₂); IR (KBr): $\tilde{v}=3299$ (s) 3232(s), 3121(s), 1691(m), 1646(s), 1504 (s), 1480(w), 1427(s), 1359(m), 1323(w), 1082(s), 1046(m), 1025(m), 866(w), 694(w), 654(w), 592(w), 526(w) cm⁻¹; Anal. calcd. for C₄H₄N₁₀: C 25.00; H 2.10; N 72.90; found: C 24.99; H 2.64; N 72.66.

2.1.3. Synthesis of (Z)-N-(8-aminobis([1,2,4]triazolo)[4,3-b:3',4'-f] [1,2,4,5]tetrazin-1(2H)- ylidene)nitramide hydrate (8· H_2O)

To nitric acid (100%, 2 mL) at -5 °C was added 7 (0.38 g, 2 mmol) in small portions. The mixture was stirred at 0 °C for 2 h and poured onto ice, the precipitate was filtered, washed with cold water (5 mL), and air dried to yield $8 \cdot \text{H}_2\text{O}$ (0.29 g, 57%) as a brown solid. T_d (onset): 166 °C. ^1H NMR (500 MHz, DMSO- d_6): $\delta = 8.6$ (br, NHNO₂), 8.3 (br, NH₂); ^{13}C NMR (125 MHz, DMSO- d_6): $\delta = 149.2$ (C = NNO₂), 148.8 (C = N), 144.7 (C-NH₂), 142.9 (C = N); IR (KBr): $\tilde{v} = 3424(\text{s})$, 3322(s), 3105(s), 2151 (w), 1656(s), 1600(s), 1544(s), 1505(s), 1445(m), 1254(s), 1167(m), 1122(m), 1060 (m), 1029(w), 994(w), 976(m), 880(w), 851(w), 779 (w), 771(w), 753(w), 713(w), 695(w), 670(w), 619(w), 561(w), 493 (m), 444(w) cm⁻¹; Anal. calcd. for $C_4H_5N_{11}O_3$: C 18.83; H 2.10; N

Scheme 1. Two failed approaches to synthesize 7.

Scheme 2. Synthesis of 7, 8, and the energetic salts (9-12).

60.38; found: C 18.65; H 2.09; N 59.34.

2.1.4. Synthesis of salts 9-12

Compound $8 \cdot H_2O$ (0.25 g, 1 mmol) was dissolved in methanol (10 mL), potassium bicarbonate solution (0.100 g, 1 mmol), or methanol solution of hydroxylamine monohydrate (0.055 mL, 1 mmol), or aqueous ammonia (0.068 mL, 1 mmol), or hydrazine monohydrate (0.049 mL, 1 mmol) and the temperature was slowly reduced to 10 °C. Then the mixture was stirred for 1 h at room temperature, the precipitate was filtered, washed with cold methanol (2 mL), and air dried to yield $9 \cdot H_2O$ -12.

Potassium (8-aminobis([1,2,4]triazolo) [4,3-b:3',4'-f] [1,2,4,5] tetrazin-1-yl)(nitro) amide hydrate (9·H₂O): Brown solid (0.28 g, 95% yield). $T_{\rm d}$ (onset): 231 °C. $^{13}{\rm C}$ NMR (300 MHz, D₂O): δ = 147.5 (C-NNO₂), 147.0 (C-NH₂), 146.9 (C = N), 145.6 (C = N); IR (KBr): \tilde{v} = 3381 (s), 2151(w), 1641(s), 1529(s), 1496(s), 1472(s), 1436(s), 1407(s), 1304 (s), 1172(m), 1093(m), 1075(m), 1024(m), 880(w), 858(w), 831(w), 773(w), 737(w), 699(w), 662(w), 615(w), 565(w), 536(w), 489(w), 440 (w) cm $^{-1}$; Anal. calcd. for C₄H₄KN₁₁O₃ : C 16.38; H 1.37; N 52.54; found: C 16.48; H 1.62; N 53.64.

Hydroxylammonium (8-aminobis([1,2,4]triazolo) [4,3-b:3',4'-f] [1,2,4,5]tetrazin -1-yl)(nitro) amide (10): Red solid (0.25 g, 93% yield). T_d (onset): 162 °C. 1 H NMR (300 MHz, d_6 -DMSO): $\delta=9.8$ (br, NH₃OH⁺), 8.5 (s, 2H, NH₂) ppm; 13 C NMR (75 MHz, d_6 -DMSO): $\delta=147.7$ (C-NNO₂), 147.3 (C-NH₂), 147.1 (C=N), 146.4 (C=N); IR (KBr): $\tilde{v}=3301(s)$, 3172(s), 2152(w), 1655(s), 1535(s), 1494(s), 1426(s), 1285(s), 1173(m), 1100(m), 1075(m), 1028(m), 1005(m), 879(m), 859 (m), 769(w), 738(w), 699(w), 665(w), 623(w), 570(w), 522(w) cm⁻¹; Anal. calcd. for C₄H₆N₁₂O₃: C 17.78; H 2.24; N 62.21; found: C 18.22; H 2.78; N 61.59.

Ammonium (8-aminobis([1,2,4]triazolo) [4,3-b:3',4'-f] [1,2,4,5] tetrazin -1-yl)(nitro) amide (11): Brown solid (0.24 g, 94% yield). $T_{\rm d}$ (onset): 224 °C. 1 H NMR (300 MHz, $d_{\rm 6}$ -DMSO): δ = 8.4 (s, 2H, NH₂), 7.2 (br, NH₄⁺); 13 C NMR (75 MHz, $d_{\rm 6}$ -DMSO): δ = 147.7 (C-NNO₂), 147.2 (C-NH₂), 147.0 (C = N), 146.4 (C = N); IR (KBr): \tilde{v} = 3189(s), 1641(s), 1526(s), 1503(s), 1427(s), 1287(s), 1171(s), 1095(s), 1080(s), 1029(s), 883(m), 861(m), 769(m), 696(w), 662(m), 620(w), 522(w), 493(w), 441(w) cm⁻¹; Anal. calcd. for C₄H₆N₁₂O₂ : C 18.90; H 2.38; N 66.13; found: C 18.54; H 2.65; N 64.26.

Hydrazinium (8-aminobis([1,2,4]triazolo) [4,3-b:3',4'-f] [1,2,4,5] tetrazin-1-yl) (nitro) amide (12): Brown solid (0.25 g, 93% yield). T_d (onset): 221 °C. ¹H NMR (300 MHz, d_6 -DMSO): δ = 8.5 (s, 2H, CNH₂), 7.3 (br, NNH₂), 3.5(br, NNH₃) ppm; 13 C NMR (75 MHz, d_6 -DMSO): δ = 147.8 (C-NNO₂), 147.3 (C-NH₂), 147.1 (C = N), 146.4 (C = N); IR (KBr): \tilde{v} = 3286(s), 3091(s), 2744(s), 2643(s), 2149(m), 1667(s), 1530(s), 1504(s), 1479(s), 1426(s), 1311(s), 1177(s), 1135(m), 1096(s), 1075(s), 1055(m), 1025(s), 967(w), 884(w), 862(m), 770(m), 696(w), 679(w), 662(m), 616(w), 544(w), 507(w), 457(w) cm⁻¹; Anal. calcd. for C₄H₇N₁₃O₂: C 17.85; H 2.62; N 67.64; found: C 17.52; H 2.77; N 65.55.

3. Results and discussion for the preparation

Two different approaches were utilized in attempts to synthesize bis ([1,2,4]triazolo)[4,3-b:3',4'-f][1,2,4,5]tetrazine-1,8-diamine, 7, (Scheme 1). Unfortunately, neither of them resulted in 7. 3,6-Bis(3,5-dimethyl-1H-pyrazol-1-yl)-1,2,4,5-tetrazine (1) [13] was treated with hydrazine monohydrate at room temperature to obtain 4, in which hydrazine substitution is at the 6 position. Treating 4 with cyanogen bromide in 1 M HCl solution gave 6-(3,5-dimethyl-1H-pyrazol-1-yl)-[1,2,4]triazolo[4,3-b][1,2,4,5]tetrazin-3-amine (5). [11] With 5 in hand, 6-hydrazinyl-[1,2,4]triazolo[4,3-b][1,2,4,5]tetrazin-3-amine (6) was prepared by a similar reaction with hydrazine monohydrate in refluxing acetonitrile. The attempts to synthesize the tricyclic compound 7 failed when 6 was reacted with cyanogen bromide in 1 M, 3 M, or concentrated HCl solution. Compound 6 was invariably recovered.

Subsequently, 3,6-dihydrazinyl-1,2,4,5-tetrazine (2) was obtained based on the literature. [12] It was reacted with cyanogen bromide in 3 M HCl solution at temperatures of 25, 50 and 70 °C, respectively, in which conditions of 25 and 50 °C gave the chloride salt of 2 (Scheme 1). When the temperature was increased to 70 °C, a yellow precipitate formed and was found to be 5,5'-diamino-3,3'-azo-1*H*-1,2,4-triazole (3). [14] A plausible route for the formation of the azo bridged triazole 3 is that 7 was formed as an intermediate but was sensitive to acid at 70 °C. Assuming that 7 was not stable in acidic solution, ethanol was used in the reaction of 2 with cyanogen bromide to obtain 7 in a yield of 75% (Scheme 2). Treating 7 with 3 M HCl at 70 °C

for 1 h gave 3 which showed that 2 is a reasonable precursor for 3. The reaction of 7 with 100% HNO $_3$ at 0 °C quenched with ice leads to the precipitate of the mono nitroimine 8 which was collected by filtration, followed by washing with water, and dried. Attempts to synthesize a nitroamine product failed. This is consistent with the aromaticity calculation (vide infra) which shows the two amino groups are not identical. By reacting 8 with bases, the ionic derivatives (9·H $_2$ O -12) were isolated in good yields (92%-95%).

4. Structure analysis

All new compounds were characterized fully by multinuclear NMR and infrared spectroscopy, as well as elemental analysis. Compounds 7–9 were further confirmed by single-crystal X-ray diffraction analysis. Suitable crystals were obtained for 7, 8, and 9 by slow evaporation of their saturated solutions in acetonitrile, methanol, and water, respectively. Crystallographic data, and data collection parameters, bond lengths, and bond angles can be found in the Supporting Information. Each of the three crystals contains one crystallographic independent molecule of 7, 8, or 9 and a co-crystallized solvent molecule of acetonitrile, methanol, or water, respectively. Compounds 7·CH₃CN and 8·CH₃OH crystallize in the monoclinic space group $P2_1/n$ with crystal densities of 1.625 g cm⁻³ and 1.713 g cm⁻³ at 100 K, respectively. Compound 9·H₂O crystallizes in the monoclinic space group CC with four molecules per unit cell and has a high density of 1.962 g cm⁻³ at 100 K although a water molecule is included. Their crystal structures are

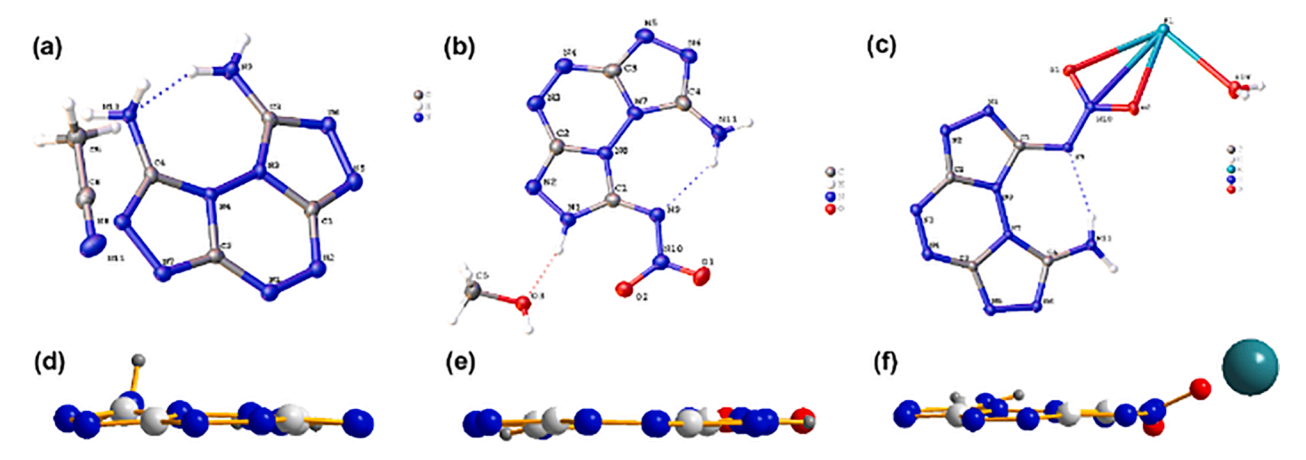


Fig. 2. Single-crystal X-ray structures of (a) (d) $7 \cdot \text{CH}_3\text{CN}$; (b) (e) $8 \cdot \text{CH}_3\text{OH}$; (c) (f) $9 \cdot \text{H}_2\text{O}$ (the molecules of solvents were deleted in (d)-(f)). The blue and red dotted lines are hydrogen bonds.

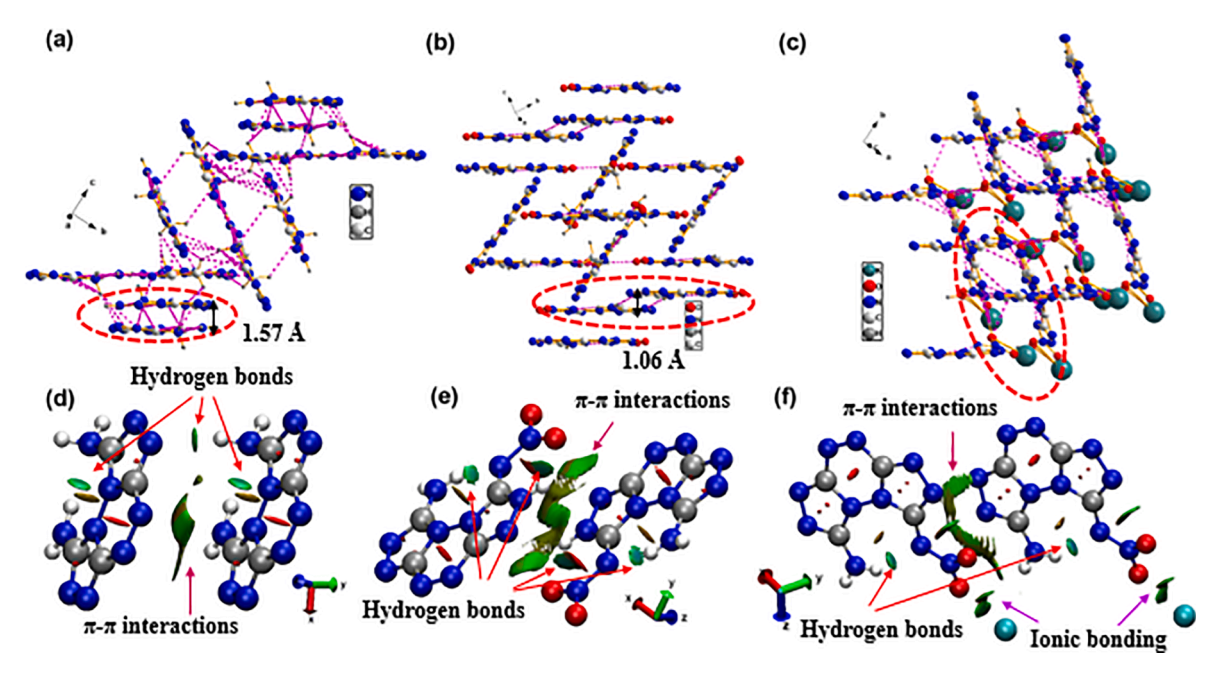


Fig. 3. (a)-(c) Packing diagram of $7 \cdot \text{CH}_3\text{CN}$ (a), $8 \cdot \text{CH}_3\text{OH}$ (b) and $9 \cdot \text{H}_2\text{O}$ (c). The hydrogen bonds are shown as pink dotted lines. (d)-(e) Noncovalent interaction analysis (blue, strong attraction; green, weak interaction; and red, strong repulsion) for 7 (d), 8 (e), and 9 (f); the original structures were extracted from the packing diagram (red ovals in Fig. 3a-3c, solvents are deleted).

shown in Fig. 2. As shown in Fig. 2(d), the left amino group is twisted out of the plane.

while the right one is in the same plane as the fused rings. However, the amino group tends to be planar after the other amino group is functionalized to the nitroimine (Fig. 2e) or nitroamine anion (Fig. 2f). Atoms N3 and N4 on the tetrazine ring of 7·CH₃CN (Fig. 2d) are twisted out of the plane with torsion angles of C1-N3-N4-C2, -5.22(14)°, N3-N4-C2-N1, 6.27(16)°. Compared with the tetrazine ring, the two triazole rings are more nearly planar (C3-N3-C1-N5, 2.06(13)°, C1-N3-C3-N6, $-1.95(12)^{\circ}$, C4-N4-C2-N7, $1.9(13)^{\circ}$, C2-N4-C4-N8, $-1.82(12)^{\circ}$) which is consistent with the aromatic analysis (vide infra) that triazole rings are more aromatic than the tetrazine ring. Among these crystals, 8 is more nearly planar than the other two. This is also indicated by the torsion angles in 8 (C4-N7-N8-C1, 8.8(12)°, N-N8-C2-N3, 1.9(2)°, N4-N3-C2-N8, $-1.7(2)^{\circ}$) are less twisted than those in 7 (C3-N3-N4-C2, $168.67(12)^{\circ}$, C1-N3-N4-C2, $-5.22(14)^{\circ}$, N3-N4-C2-N1 $6.27(16)^{\circ}$) and ${\bf 9}$ $(C3-N7-N8-C1\ 175.0(3)^{\circ},\ C3-N7-N8-C2,\ -3.8(3)^{\circ},\ N7-N8-C2-N3,\ 3.8$ (4)°). Good planarity is helpful in enhancing the density of the corresponding compound.

The packing diagrams of $7 \cdot \text{CH}_3\text{CN}$, $8 \cdot \text{CH}_3\text{OH}$, and $9 \cdot \text{H}_2\text{O}$ are shown in Fig. 3 (a-c), in which $7 \cdot \text{CH}_3\text{CN}$ shows mixed stacking, $8 \cdot \text{CH}_3\text{OH}$ is "Z" shaped, and $9 \cdot \text{H}_2\text{O}$ exhibits net arrangement, respectively. Additionally, intermolecular and intramolecular hydrogen bonds are marked as pink dotted lines; the details of these hydrogen bonds are given in the Supporting Information. These extensive hydrogen-bonding interactions form complex 3D networks within the structures of 7-9, which make an important contribution to enhance the thermal stabilities of the complexes. $\pi - \pi$ stacking types are observed in these packing diagrams. To obtain more information on intra- and intermolecular effects on crystal packing comprehensively, two face-to-face molecular diagrams were studied by noncovalent interaction analysis, which is an invaluable approach to identify noncovalent interactions based on the analysis of electron density and the reduced density gradient. [15]

The geometries of **7–9** were optimized using the ORCA 3.0 program. [16] The noncovalent interactions plots were calculated using Multiwfn [17] and visualized by the Visual Molecular Dynamics program. [18]

Table 1
Properties of energetic compounds (7–12).

| Comp. | $T_{\mathbf{d}}^{\mathbf{a}}(^{\circ}\mathbf{C})$ | $ ho^{\mathrm{b}}(\mathrm{g~cm^{-3}})$ | $\Delta_{\rm f} H^{\circ c}({\rm kJ~g}^{-1})$ | N ^d (%) | $v_{\rm D}^{\rm e}({\rm m~s}^{-1})$ | $P^{f}(GPa)$ | $IS^{g}(J)$ | FS ^h (N) | $I_{\rm sp}^{\rm i}({\rm s})$ |
|----------------|---|--|---|--------------------|-------------------------------------|--------------|------------------|---------------------|-------------------------------|
| 7 | 247 | 1.76 | 4.27 | 72.9 | 8544 | 27.3 | >40 | >360 | 233 |
| $8 \cdot H_2O$ | 166 | 1.88 | 2.41 | 65.0 | 9073 | 34.0 | >40 | >360 | 236 |
| $9 \cdot H_2O$ | 231 | 1.97 | 0.78 | 56.0 | 8065 | 26.5 | >40 | >360 | 190 |
| 10 | 162 | 1.83 | 2.35 | 62.2 | 8917 | 31.9 | >40 | >360 | 234 |
| 11 | 224 | 1.75 | 2.32 | 66.1 | 8410 | 26.7 | >40 | >360 | 220 |
| 12 | 221 | 1.84 | 2.72 | 67.6 | 9088 | 32.3 | >40 | >360 | 230 |
| RDX | 205 | 1.81 | 0.36 | 37.8 | 8748 | 34.9 | 7.4 ^j | 120 | _ |
| HMX | 280 | 1.90 | 0.25 | 37.8 | 9144 | 39.2 | 7.4 | 120 | - |

- ^a Decomposition temperature (onset) under nitrogen (DSC, 5 °C min^{−1}).
- ^b Density measured by gas pycnometer (25 °C).
- ^c Heat of formation.
- $^{\rm d}$ Nitrogen content.
- ^e Detonation pressure (calculated with Explo5 v6.01).
- f Detonation velocity (calculated with Explo 6.01).
- ^g Impact sensitivity.
- h Friction sensitivity.
- ⁱ Specific impulse (values obtained from Explo5 v6.01 and calculated at an isobaric pressure of 70 bar and initial temperature of 3300 K. The expansion conditions are equilibrium expansion).
- j Idaho expt'l value.

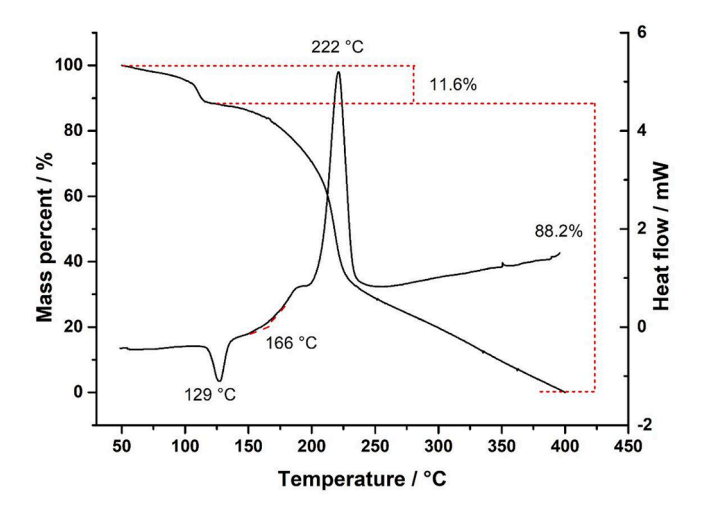


Fig. 4. TGA and DSC curves of $8 \cdot \rm{H_2O}$ under nitrogen with a heating rate of 5 $^{\circ}\rm{C}~min^{-1}.$

The results are given in Fig. 3 (d)-(f), where there are red isosurfaces located inside the triazole and tetrazine rings which denote steric repulsion in the ring. Blue and green isosurfaces can be identified on the edge, indicating that the dimeric stabilization is dominated by hydrogen bonds and π - π stacking interactions. In addition, deep green isosurfaces were also observed in compound 9, which is dominated by ionic bonding. Isosurfaces for edge-to-face π - π stacking are observed around the tetrazine and triazole rings, indicating that the fused ring system contributes to form π - π stacking interactions. It is obvious that compound 8 exhibits considerably more π - π interactions than 7, which also promotes the closer packing of molecules of 7 (1.57 Å), and subsequently shows a higher density. These intense hydrogen bonds and π - π stacking interactions are expected to give excellent thermal stabilities and low sensitivities towards impact and friction to compounds 7–9.

5. Physical and detonation properties

To obtain a comprehensive evaluation as high energy dense materials, the physiochemical properties of the new tricyclic compounds were determined and are listed in Table 1. Differential scanning calorimetry (DSC) of **7–12** was carried out to determine their thermal behavior at a heating rate of 5 °C min⁻¹ over the temperature range from

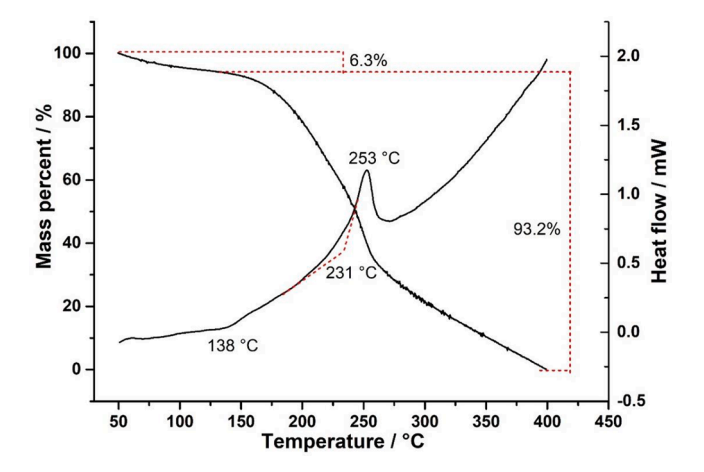


Fig. 5. TGA and DSC curves of $9 \cdot H_2O$ under nitrogen with a heating rate of 5 $^{\circ}C$ min $^{-1}$.

 $50~^{\circ}\text{C}$ to $400~^{\circ}\text{C}$ in a dry nitrogen atmosphere. All of the new energetic compounds in Table 1 decompose without melting. Except for the nitramines 8·H₂O (166 °C) and 10 (162 °C); the energetic ditriazole-1,2,4,5tetrazinanes exhibit favorable decomposition temperatures ranging from 221 to 247 °C. In the DSC and TGA plots of $8 \cdot H_2O$ (Fig. 4), thermal decomposition shows two decomposition steps. The first step occurs at 115 °C accompanied with a mass loss of 11.6%, which indicates the loss of water and slight decomposition. As shown in Fig. 5, 9·H₂O exhibits two steps of weight loss in which 6.3% is corresponding to the loss of water. Density, a determining factor of energy level, was measured using a gas pycnometer at 25 °C. The experimentally determined densities fall between 1.75 and 1.97 g \mbox{cm}^{-3} , and most meet the density requirement for new high energy dense materials (1.80–2.0 g cm⁻³). Compound 7 is featured with excellent thermal behavior (261 °C) supported by calculated aromaticity and the π - π stacking interactions and hydrogen bonds of the crystal packing diagram. Unfortunately, its density (1.76 g cm⁻³) is not as high as expected for a fused ring compound which likely results from the fact that not all the atoms are coplanar as seen from the crystal structures.

Heats of formation $(\Delta_f H^\circ)$ of tricyclic compounds were computed by using the Gaussian 03 (Revision E.01) suite of programs. [10] Benefitting from ring-strain energy of the fused backbone and a large number of N-N or N = N bonds within the molecule, all tricyclic compounds have

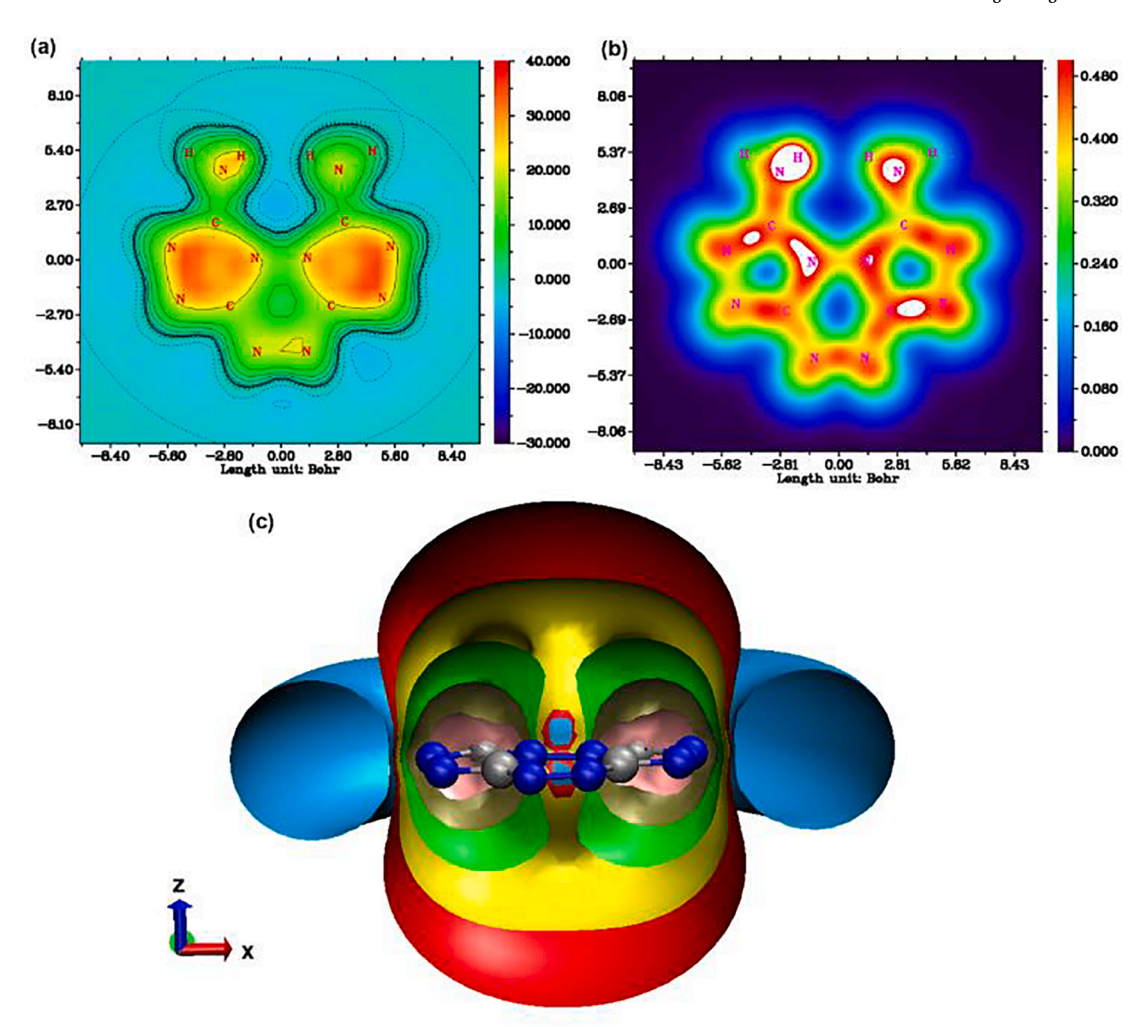


Fig. 6. (a) Shielding map of **7**. (b) Pathway of electron delocalization (1.2 Bohr above the XY plane). (c) Clipping plane for multiple *iso*-chemical shielding surfaces (shielding surfaces at −1 ppm in cyan, at 2 ppm in red, at 4 ppm in yellow, at 8 ppm in green, 16 ppm in tan; and 32 ppm in pink, viewing in the XZ plane).

positive $\Delta_f H^\circ$ values ranging from 0.78 to 4.27 kJ g⁻¹, which are all larger than those of RDX (0.36 kJ g^{-1}) and HMX (0.25 kJ g^{-1}). The nitrogen percentages of compounds 7-12 fall in the range of 56.0 to 72.9%, which are much higher than those of RDX and HMX (37.8%). With experimental densities and calculated heats of formation in hand, detonation properties of 7-12 were obtained by employing the EXPLO5 computer code (Version 6.01). [19] The results are summarized in Table 1, compounds 8 and 12 exhibit better detonation velocities (ν_D , 8, 9073 m s⁻¹; **12**, 9088 m s⁻¹) and detonation pressures (P, **8**, 34.0 GPa; 12, 32.3 GPa) than RDX (ν_D , 8748 m s⁻¹; P, 34.9 GPa), and comparable with those of HMX (ν_D , 9144 m s⁻¹; P, 39.6 GPa). Detonation properties of 8 and 12 significantly outperform those of other ditriazolo-1,2,4,5tetrazines (7, and 9-11) owing to the advantage of high densities and heats of formation. Compound 7 exhibits a detonation velocity of 8544 m s⁻¹ and pressure of 27.3 GPa, which is slightly lower than those of RDX. All new energetic compounds 7–12 are insensitive towards impact and friction, which indicates that the good aromaticity, hydrogen bonds and π - π interactions in the structures significantly contribute to enable the lower the mechanical stimuli. The specific impulse (I_{sp}) , an important measure of a propellant's efficiency (in seconds), was also calculated (Explo 5 v6.01) for 7-12. These values ranged from 190 to 236 s which, except for the potassium salt 9, are higher than that of ADN (202 s).

6. The computation investigation of aromaticity for 7

Evaluation of the overall aromaticity of 7, a tricyclic framework assembling aromatic triazoles and a non-aromatic tetrazine, is of considerable interest in order to understand the intrinsic structure–property relationships. Nucleus-independent chemical shift (NICS) [20,21] and isochemical shielding surfaces (ICSS) [22,23] were employed to calculate the magnetic properties of 7 by using Gaussian03 (Revision E.01) suite of programs [10] and the Multiwfn program (Version 3.3.9). [17] Generally, the original definition of the NICS is the negative value of the absolute magnetic shielding computed at ring centers. [24] NICSzz shows a two dimensional grid of lattice points around the molecule which offers an improved interpretation of aromaticity with fewer errors. To investigate the shielding distribution of the zz component 1 Å above the plane, the NICS of 125,000 points around the molecule 7 was computed. Color-filled shielding maps are sketched and are shown in Fig. 6 (a). The colors range from -30

to + 40 ppm with dark blue denoting extreme anti-shielding regions and red denoting the shielding regions. Considering that shielding and NICS share the same value of opposite sign, a darker red color indicates the structure has better aromaticity. The curves in the picture are contour lines and the scale on the right refers to the shielding of a zz component. Fig. 6(a) has two triazole rings which are filled with red, which shows strong aromaticity. Conversely, the tetrazine ring is not aromatic. It is interesting that the two amino groups show different aromaticities, in which only one of them is conjugated with the adjacent

triazole ring, thus showing weak aromaticity.

To understand the aromaticity of 7, ICSS around the magnetically anisotropic moieties were also studied, in which both direction and scale of the anisotropy effect can be quantified. Actually, an ICSS calculation is that the magnetic anisotropy effect of unsaturated chemical bonds and the ring current effect in arenes are calculated quantitatively as NICSs in a three dimensional grid of lattice points around the molecule. A pathway of electron delocalization is visualized by employing localized orbital locator (LOL) analysis (Fig. 6b). [25] Unlike NICSs which are the negative values of the absolute magnetic shielding, ICSS shows the value of the magnetic shielding at different positions directly. The colors range from 0 to 0.48 ppm with dark blue and red regions. The white regions have shielding values>0.48 ppm. The delocalized electron clouds are found in all the atoms of 7 which form a distinct π -electron conjugate path. A clipping plane of multiple iso-chemical shielding surfaces (ICSS = -1, 2, 4, 8, 16, and 32 ppm, respectively) is plotted by Visual Molecular Dynamics (Version 1.9.3) (Fig. 6c).[18] The shielding surfaces cover all the molecule when ICSS is less or equal to 4 ppm, indicating a favorable overall aromaticity. This is expected to enhance the thermostability of 7. An ICSS of 8 ppm (Fig. 6c, green shielding surface) covers the two triazole rings but only parts of the tetrazine ring, which means the aromaticity of the triazoles is relatively superior to that of tetrazine. The stronger aromaticity of triazoles is clearer as the ICSS grows. It is interesting that ICSS of 16 and 32 ppm covers the right triazole more than the left one, which indicates that the right triazole is more strongly aromatic than the left one. Combined with the result from NICS, it can predict that two amino groups attached to triazoles have different chemical properties which agrees with experiment.

7. Conclusion

In conclusion, a new family of fused tricyclic ditriazolo-1,2,4,5tetrazine derivatives was designed and synthesized. The structures were fully characterized by using ¹H, and ¹³C NMR and IR spectroscopy, and elemental analysis, as well as differential scanning calorimetry. Compounds 7·CH₃CN, 8·CH₃OH, and 9·H₂O were further confirmed by X-ray diffraction. The facile and concise cyclization was accomplished by reacting 6-dihydrazinyl-1,2,4,5-tetrazine (2) with cyanogen bromide in ethanol. The nucleus-independent chemical shift (NICS) and isochemical shielding surfaces (ICSS) analyses indicate that 7 has high aromaticity. The two triazole rings are more aromatic than the tetrazine ring, which is consistent with the crystal structure of 7, in which both triazole rings are more planar than the tetrazine ring. Face-to-face π - π stacking and a large number of hydrogen bonds were observed in crystals 7·CH₃CN, 8·CH₃OH, and 9·H₂O, which are helpful in increasing the thermal stabilities and lower sensitivities towards impact and friction of the corresponding compounds. Compounds 7 and 12 show excellent decomposition temperatures, high nitrogen content, good detonation properties (moderate for 7), and are insensitive to mechanical stimuli, which are comparable with those of RDX and HMX, respectively.

Declaration of Competing Interest

The authors declare that they have no known competing financial interests or personal relationships that could have appeared to influence the work reported in this paper.

Acknowledgements

The Rigaku Synergy S Diffractometer was purchased with support from the MRI program by the National Science Foundation Grant No. 1919565.

Appendix A. Supplementary data

Supplementary data to this article can be found online at https://doi.

org/10.1016/j.cej.2021.133235.

References

- [1] M. Reichel, D. Dosch, T.M. Klapötke, K. Karaghiosoff, The correlation between structure and energetic properties of three nitroaromatic compounds: bis(2,4dinitrophenyl) ether, bis(2,4,6-trinitrophenyl) ether and bis(2,4,6-trinitrophenyl) thioether, J. Am. Chem. Soc. 141 (2019) 19911–19916.
- [2] Y. Wang, Y. Liu, S. Song, Z. Yang, X. Qi, K. Wang, Y. Liu, Q. Zhang, Y. Tian, Accelerating the discovery of insensitive high-energy-density materials by a materials genome approach, Nat. Commun. 9 (2018) 2444.
- [3] T.M. Klapötke, P.C. Schmid, S. Schnell, J. Stierstorfer, 3,6,7-Triamino-[1,2,4] triazolo[4,3-b][1,2,4]triazole: a non-toxic, high-performance energetic building block with excellent stability, Chem. Eur. J. 21 (2015) 9219–9228.
- [4] M.H.V. Huynh, M.A. Hiskey, D.E. Chavez, D.L. Naud, R.D. Gilardi, Synthesis, characterization, and energetic properties of diazido heteroaromatic high-nitrogen C-N compound, J. Am. Chem. Soc. 127 (36) (2005) 12537–12543.
- [5] P. Yin, J. Zhang, L.A. Mitchell, D.A. Parrish, J.M. Shreeve, 3,6-Dinitropyrazolo[4,3-c]pyrazole-based multipurpose energetic materials through versatile N-functionalization strategies, Angew. Chem. Int. Ed. 128 (41) (2016) 13087–13089.
- [6] M.S. Klenov, A.A. Guskov, O.V. Anikin, A.M. Churakov, Y.A. Strelenko, I. V. Fedyanin, K.A. Lyssenko, V.A. Tartakovsky, Synthesis of tetrazino-tetrazine 1,3,6,8-tetraoxide (TTTO), Angew. Chem. Int. Ed. 55 (38) (2016) 11472–11475.
- [7] Y. Tang, D. Kumar, J.M. Shreeve, Balancing excellent performance and high thermal stability in a dinitropyrazole fused 1,2,3,4-tetrazine, J. Am. Chem. Soc. 139 (2017) 13684–13687.
- [8] D.G. Piercey, D.E. Chavez, B.L. Scott, G.H. Imler, D.A. Parrish, An energetic triazolo-1, 2, 4-triazine and its N-oxide, Angew. Chem. Int. Ed. 55 (49) (2016) 15315–15318.
- [9] P. Yin, J. Zhang, G.H. Imler, D. Parrish, J.M. Shreeve, Polynitro-functionalized dipyrazolo-1,3,5-triazinanes: energetic polycyclization toward high density and excellent molecular stability. Angew. Chem. Int. Ed. 56 (2017) 8834–8838.
- [10] M.J. Frisch, G.W. Trucks, H.G. Schlegel, G.E. Scuseria, M.A. Robb, J. A. Montgomery, T. Jr, K.N. Vreven, J.C. Kudin, J.M. Burant, S.S. Millam, J. Iyengar, V. Tomasi, B. Barone, M. Mennucci, G. Cossi, N. Scalmani, G.A. Rega, H. Petersson, M. Nakatsuji, M. Hada, K. Ehara, R. Toyota, J. Fukuda, M. Hasegawa, T. Ishida, Y. Nakajima, O. Honda, H. Kitao, M. Nakai, X. Klene, J.E. Li, H.P. Knox, J. B. Hratchian, V. Cross, C. Bakken, J. Adamo, R. Jaramillo, R.E. Gomperts, O. Stratmann, A.J. Yazyev, R. Austin, C. Cammi, J.W. Pomelli, P.Y. Ochterski, K. Ayala, G.A. Morokuma, P. Voth, J.J. Salvador, V.G. Dannenberg, S. Zakrzewski, A.D. Dapprich, M.C. Daniels, O. Strain, D.K. Farkas, A.D. Malick, K. Rabuck, J. B. Raghavachari, J.V. Foresman, Q. Ortiz, A.G. Cui, S. Baboul, J. Clifford, B. B. Cioslowski, A.L.G. Stefanov, P. Liu, I. Piskorz, R.L. Komaromi, D.J. Martin, T. Fox, M.A. Keith, C. Allaham, A. Peng, M.C. Nanayakkara, P.M.W. Gill, B. Johnson, W. Chen, M. Wong, C. Gonzalez, J.A. Pople, Gaussian 03, revision E.01; Gaussian Inc: Wallingford, CT. (2004).
- [11] D.E. Chavez, M.A. Hiskey, Synthesis of the bi-heterocyclic parent ring system 1,2,4-triazolo[4,3-b][1,2,4,5]tetrazine and some 3,6-disubstituted derivatives, J. Heterocycl. Chem. 35 (1998) 1329-1332.
- [12] Y.-H. Gong, F. Miomandre, R. Méallet-Renault, S. Badré, L. Galmiche, J. Tang, P. Audebert, G. Clavier, Synthesis and physical chemistry of s-tetrazines: which ones are fluorescent and why? Eur. J. Org. Chem. 2009 (2009) 6121–6128.
- [13] M.D. Coburn, G.A. Buntain, B.W. Harris, M.A. Hiskey, K.Y. Lee, D.G. Ott, An improved synthesis of 3,6-diamino-1,2,4,5-tetrazine. II. From triaminoguanidine and 2,4-pentanedione, J. Heterocycl. Chem. 28 (1991) 2049-2050.
- [14] Q. Yu, R.J. Staples, J.M. Shreeve, An azo-bridged triazole derived from tetrazine, Z. Anorg. Allg. Chem. 646 (22) (2020) 1799–1804.
- [15] E.R. Johnson, S. Keinan, P. Mori-Sánchez, J. Contreras-García, A.J. Cohen, W. Yang, Revealing noncovalent interactions, J. Am. Chem. Soc. 132 (18) (2010) 6498–6506.
- [16] F. Neese, The ORCA program system, WIREs Comput. Mol. Sci. 2 (1) (2012) 73–78.
- [17] T. Lu, F. Chen, Multiwfn: a multifunctional wavefunction analyzer, J. Comput. Chem. 33 (2012) 580–592.
- [18] W. Humphrey, A. Dalke, K. Schulten, VMD: visual molecular dynamics, J. Mol. Graph. Model. 14 (1996) 33–38.
- [19] M. Sućeska, EXPLO5, 6.01; Brodarski Institure: Zagreb, Croatia. 2013.
- [20] T.M. Krygowski, B.T. Stępień, M.K. Cyrański, K. Ejsmont, Relation between resonance energy and substituent resonance effect in *P*-phenols, J. Phys. Org. Chem 18 (8) (2005) 886–891.
- [21] P.v.R. Schleyer, C. Maerker, A. Dransfeld, H. Jiao, N.J.v.E. Hommes, Nucleusindependent chemical shifts: a simple and efficient aromaticity probe, *J. Am. Chem.* Soc. 118 (1996) 6317-6318.
- [22] S. Klod, E. Kleinpeter, Ab initio calculation of the anisotropy effect of multiple bonds and the ring current effect of arenes-application in conformational and configurational analysis, J. Chem. Soc., Perkin Trans. 2 (2001) 1893–1898.
- [23] Z. Liu, T. Lu, Q. Chen, An sp-hybridized all-carboatomic ring, cyclo[18]carbon: bonding character, electron delocalization, and aromaticity, Carbon 165 (2020) 468–475.
- [24] Y. Wang, S. Li, Y. Li, R.B. Zhang, D. Wang, S. Pang, A comparative study of structure, energetic performance and stability of nitro-NNO-azoxy substituted explosives, J. Mater. Chem. A 2 (2014) 20806–20813.
- [25] Heiko Jacobsen, Localized-orbital locator (LOL) profiles of chemical bonding, Can. J. Chem. 86 (7) (2008) 695–702.